THE ASTROPHYSICAL JOURNAL, 344:57–74, 1989 September 1

GROUPS OF GALAXIES IN THE CENTER FOR ASTROPHYSICS REDSHIFT SURVEY[1]

MASSIMO RAMELLA[2]
Osservatorio Astronomico di Trieste
AND
MARGARET J. GELLER AND JOHN P. HUCHRA
Harvard-Smithsonian Center for Astrophysics
Received 1988 November 8; accepted 1989 February 1

ABSTRACT

We apply an objective group identification algorithm described by Huchra and Geller to the Center for Astrophysics redshift survey complete to $m_{B(0)} = 15.5$ over the right ascension range $8^h \leq \alpha \leq 17^h$ and declination range $26.°5 \leq \delta < 38.°5$. We extract a catalog of 128 groups with three or more members; 92 of these groups constitute our "statistical sample." Simulations of the geometry of large-scale structure indicate that $\gtrsim 30\%$ of the groups with three or four members are probably an artifact of the geometry.

The median velocity dispersion for the 36 groups in the "statistical sample" with five or more members is $\sigma_v = 228$ km s^{-1}, and the median $M/L_{B(0)}$ is $178h\ M_\odot/L_\odot$, where the Hubble constant H_0 is $100h$ km s^{-1} Mpc^{-1} (we take $h = 1$ unless otherwise indicated). The median parameters for the 92 group sample are similar. The sample contains seven Abell clusters; the physical properties of these clusters overlap substantially with those of groups. In fact, the distinction between groups and clusters is not generally apparent on the basis of selection of systems in redshift space.

Comparison of the distribution of group centers with the distribution of all of the galaxies in the survey shows qualitatively that groups trace the large-scale structure in the region. The physical properties of groups may be related to the details of the large-scale structure. Groups reextracted from the earlier CfA survey complete to $m_{B(0)} = 14.5$ have a significantly lower median velocity dispersion, $\sigma_v = 131$ km s^{-1}, than the groups in the 15.5 survey.

About 58% of the groups in the $m_{B(0)} \leq 15.5$ survey contains three or more galaxies brighter than L^*, the characteristic luminosity in the Schechter form of the luminosity function; in contrast, 77% of the groups in the 14.5 survey have fewer than three members brighter than L^*. The difference in the group catalogs is probably largely a result of the properties of large-scale structures and their location relative to the survey limits.

Subject headings: galaxies: clustering — galaxies: redshifts

I. INTRODUCTION

Studies of the dynamics of systems of galaxies—from small groups to rich clusters—have long provided evidence for dark matter in the universe (Zwicky 1933; Rood, Rothman, and Turnrose 1970; Faber and Gallagher 1979). For groups of galaxies, there are substantial uncertainties in the determination of mass-to-light ratios. Some problems arise in the identification and statistical analysis of groups; others reflect deeper issues in understanding the relative distribution of dark and light-emitting matter in the universe.

Approaches to the construction of catalogs of groups of galaxies have become increasingly objective and more closely related to the physics of systems of galaxies. In early catalogs (e.g., Holmberg 1969; de Vaucouleurs 1975) groups were selected primarily by visual inspection of plates. In the absence of complete redshift surveys, Turner and Gott (1976) first used an objective algorithm to extract groups from a catalog of the positions of galaxies in the sky. With the increasing availability of extensive redshift surveys, the focus has now shifted to the objective identification of groups of galaxies from these three-dimensional data (Materne 1978, 1979; Tully 1980; Huchra and Geller 1982, hereafter HG82; Press and Davis 1982; Geller and Huchra 1983, hereafter GH83; Vennik 1984; Tully 1987; Nolthenius and White 1987, hereafter NW). Even in objectively constructed group catalogs, group mass-to-light ratios range over 3 orders of magnitude. Perhaps more sobering, the median mass-to-light ratios varies by more than a factor of 2 from one catalog to another. Heisler, Tremaine, and Bahcall (1985) and NW conclude that the large range and variation in median mass-to-light ratio are probably unavoidable statistical problems which result from studying systems with small numbers of members.

The detailed properties of the groups in any catalog are a function of (1) the galaxy survey, (2) the general characteristics of the larger scale structure in which groups of galaxies are embedded, and (3) the algorithm applied to select groups. Here we examine groups in two slices of the Center for Astrophysics redshift survey extension. The catalog of 1766 galaxies covers the right ascension range $8^h \leq \alpha \leq 17^h$ and the declination range $26.°5 \leq \delta < 38.°5$ (Fig. 1). The large-scale structure in the region is characterized by voids surrounded (or nearly surrounded) by thin surfaces (FWHM $\simeq 500$ km s^{-1}). The set of systems of galaxies included in this survey differs from earlier surveys in the inclusion of more rich clusters; there are seven Abell clusters in the region. The extension of systems of galaxies along the line of sight ("fingers" in redshift space) produces distortion of a map in redshift space relative to its

[1] Research reported here based in part on observations made with Multiple Mirror Telescope, a joint facility of the Smithsonian Astrophysical Observatory and the University of Arizona.
[2] Also Harvard-Smithsonian Center for Astrophysics.

counterpart in real three-dimensional space. These distortions are obvious for rich systems like the Coma Cluster which have a velocity dispersion large compared with the typical FWHM of the extended sheets in the survey (see Fig. 1). The distortions caused by small groups of galaxies with a typical line-of-sight velocity dispersion of $\lesssim 200$ km s^{-1} (Rood and Dickel 1978; HG82; Tully 1987) are more subtle.

We identify groups of galaxies in the survey by applying the percolation algorithm originally suggested by HG82. In order to examine the impact of large-scale structure on group identification, we also apply the algorithm to a geometric model for the structure in the region. Comparison of this model with the data suggests that at least a third of the sample of groups with three or four members are spurious—they are merely an "accident" of the geometry of large-scale structure. The "pseudogroups" have reasonable physical parameters because the FWHM of the sheets is about twice the velocity dispersion of a typical group. At the same time that the geometry causes contamination of a group catalog, it also enables identification of the system with little foreground/background contamination. The existence of voids with diameters large compared with the FWHM of the structures suppresses the number of velocity interlopers.

We review the group finding algorithm in § II. We discuss the survey in § III. Section IV is a discussion of the optimization of the selection parameters for the group finding algorithm, and § V describes the group catalog. We examine the physical properties of groups in § VI. We compare the properties of groups with the properties of the Abell clusters in the survey with the properties of groups identified in the earlier CfA survey complete to $m_{B(0)} = 14.5$. We also qualitatively examine the role of groups as tracers of large-scale structure. Section VII summarizes the results and their implications.

II. THE ALGORITHM

We use the group finding algorithm described in HG82. Here we summarize the main features.

The cluster algorithm identifies isodensity contours of the galaxy distribution in a magnitude-limited sample. We start with a galaxy which has not yet been assigned to a group. We then search around it for companions with projected separation

$$D_{12} \leq D_L(V_1, V_2, m_1, m_2) \quad (1)$$

and with line-of-sight velocity difference

$$V_{12} \leq V_L(V_1, V_2, m_1, m_2), \quad (2)$$

where V_1 and V_2 are the redshifts of the galaxy and its companion; m_1 and m_2 are their magnitudes. We add companions to the list of group members. Then we search the surroundings of each companion. We repeat the loop until we can identify no further members. This completely objective algorithm is commutative and produces a unique catalog.

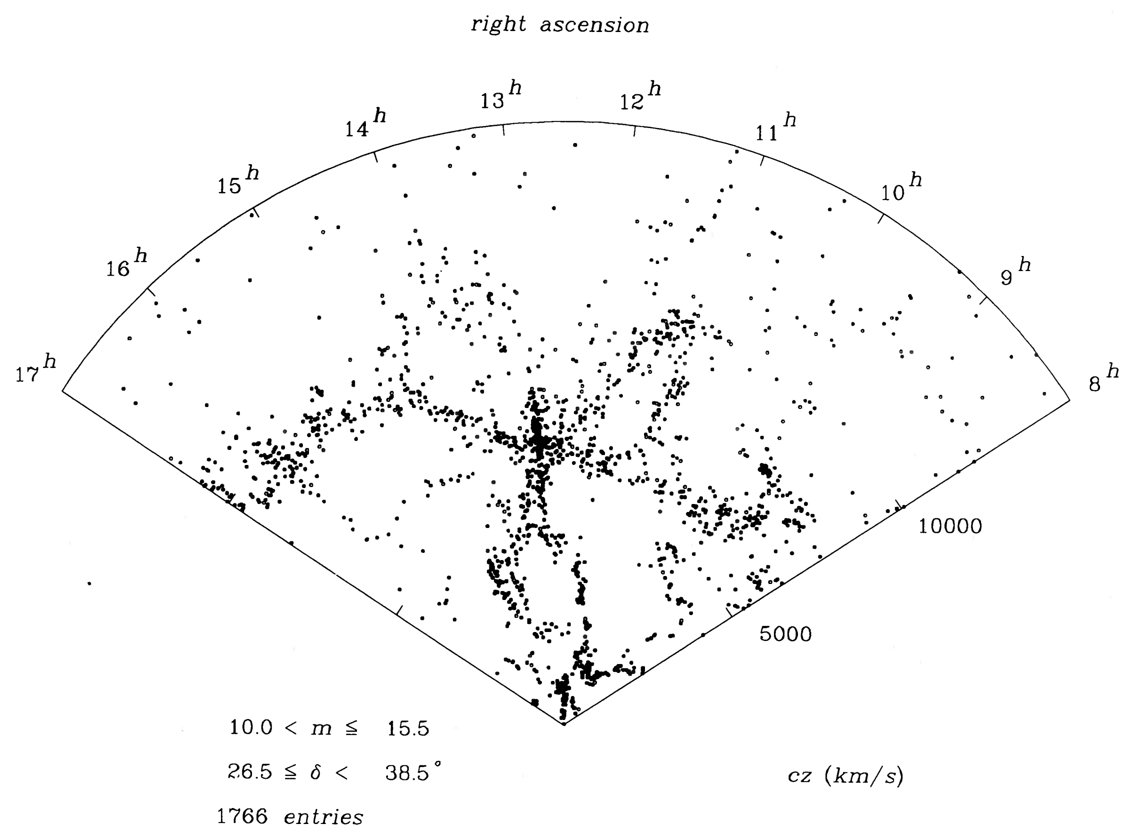

FIG. 1.—Cone diagram for the declination range $26°.5 \leq \delta < 38°.5$. The plot contains 1766 galaxies with $m_{B(0)} \leq 15.5$ and $cz \leq 15{,}000$ km s^{-1}.

To account for the variation in the sampling of the galaxy luminosity function, $\phi(M)$, with distance, we scale the parameter D_L according to

$$D_L = D_0 R , \tag{3}$$

where

$$R = \left[\int_{-\infty}^{M_{12}} \Phi(M) dM \Big/ \int_{-\infty}^{M_{\rm lim}} \Phi(M) dM \right]^{-1/2} , \tag{4}$$

$$M_{\rm lim} = m_{\rm lim} - 25 - 5 \log (V_f/H_0) , \tag{5}$$

$$M_{12} = m_{\rm lim} - 25 - 5 \log [(V_1 + V_2)/2H_0] , \tag{6}$$

and D_0 is the selection parameter at a fixed fiducial redshift V_f. We scale V_L in the same way as D_L; thus the ratio D_L/V_L is constant.

The number density contour surrounding a group corresponds to a fixed enhancement above the global mean number density of

$$\frac{\delta\rho}{\rho} = \frac{3}{4\pi D_0^3} \left[\int_{-\infty}^{M_{\rm lim}} \Phi(M) dM \right]^{-1} - 1 . \tag{7}$$

For each of the groups we derive the following set of physical characteristics. The virial radius is

$$R_h = \frac{\pi V}{H_0} \sin \left\{ \frac{1}{2} \left[\frac{N_{\rm mem}(N_{\rm mem} - 1)}{2} \left(\sum_i \sum_{j>i} \theta_{ij}^{-1} \right)^{-1} \right] \right\} , \tag{8}$$

where V is the mean velocity of the group, $N_{\rm mem}$ is the number of group members, and θ_{ij} is the angular separation of group members i and j. The mean projected separation is

$$R_p = \frac{8V}{\pi H_0} \sin \left[\frac{1}{N_{\rm mem}(N_{\rm mem} - 1)} \sum_i \sum_{j>i} \theta_{ij} \right] . \tag{9}$$

The virial mass is

$$M_v = 6\sigma_v^2 R_h/G , \tag{10}$$

and the virial crossing time (in units of the Hubble time) is

$$t_c = \frac{3}{5^{3/2}} \frac{R_h H_0}{\sigma_v} , \tag{11}$$

where σ_v is the line-of-sight velocity dispersion of the group. These definitions agree with those in GH83 and with NW [except that the crossing time in NW is $t_c = (2/\sqrt{3}) R_h H_0/\sigma_v$].

III. THE REDSHIFT SURVEY AND LUMINOSITY FUNCTION

We apply the group finding algorithm to the first two complete strips of the Center for Astrophysics redshift survey extension (Huchra *et al.* 1989). The redshift survey contains 1766 galaxies with $m_{B(0)} \leq 15.5$ in the Zwicky-Nilson merged catalog and within the limits $8^{\rm h} \leq \alpha \leq 17^{\rm h}$, $26\overset{\circ}{.}5 \leq \delta < 38\overset{\circ}{.}5$. The sample covers 0.42 sr of the sky. The sample we analyze includes only the galaxies with $cz \leq 15{,}000$ km s^{-1}. We apply the algorithm in the declination range $26\overset{\circ}{.}5 \leq \delta < 32\overset{\circ}{.}5$ (*6° slice*) and to the full *12° slice*. The velocities are *not* corrected for Virgocentric flow. At the depth of this slice, the correction has a completely negligible effect on the results.

The luminosity function we use to scale the selection parameters D_0 and V_0 is from de Lapparent, Geller, and Huchra (1988) and is consistent with the more detailed analysis by de Lapparent, Geller, and Huchra (1989; see Table 1 of their paper). Magnitudes are on the Zwicky $B(0)$ system, and we make no absorption correction. We parameterize the luminosity function with the Schechter (1976) form with

$$\phi^* = 0.025 \text{ galaxies mag}^{-1} \text{ Mpc}^{-3};$$

$$M^*_{B(0)} = -19.15; \quad \alpha = -1.2 . \tag{12}$$

The corresponding luminosity density is 2.05×10^8 $L_\odot$ Mpc^{-3}. Thus $\Omega = 1$ for a critical mass-to-light ratio $M/L_{B(0)} = 1360\ M_\odot/L_\odot$.

IV. TUNING THE SEARCH ALGORITHM

Several requirements dictate the choice of the two selection parameters D_0 and V_0. The choices should minimize the number of interlopers without biasing the velocity dispersion toward artificially low values. The choice of selection parameters should also maximize the identification of real physical systems relative to accidental superpositions. In other words, we seek to identify regions where the Hubble flow is distorted by condensations of galaxies. For virialized systems, the distortion has the characteristic form of an extension or "finger" along the line of sight. The distorted density enhancements in redshift space correspond to density enhancements in real three-dimensional space.

In the redshift survey slices, groups and clusters of galaxies are embedded in thin sheetlike structures (FWHM $\lesssim$ 500 km s^{-1}; de Lapparent 1986; Geller 1987). Even without gravitational distortion, the group finding algorithm will identify condensations in a geometry where galaxies are randomly distributed in thin sheets which surround (or nearly surround) voids. These "pseudogroups" will contaminate a catalog drawn from the survey.

To examine the degree of contamination and the properties of the "pseudogroups," we apply the selection algorithm to a simulation of the 6° slice. In this simulation (de Lapparent 1986) points are first randomly distributed. The simulation is magnitude-limited and has the luminosity function parameters appropriate for the data. Then we remove points in spherical voids with diameters comparable to those in the data until the fraction of the volume filled by the points is comparable to the volume filled by the galaxies in the survey (~20%). In this simulation there is no gravitational distortion of the distribution of points.

To explore the consequences of various choices of the parameters, we produce a set of catalogs for both sets of data and for the simulation. In all catalogs, the groups have mean velocities $cz \leq 12{,}000$ km s^{-1}; members may have velocities as large as 15,000 km s^{-1}.

a) The Parameter D_0 and the Density Enhancement

We produce group catalogs at density enhancements $\delta\rho/\rho$ of 20, 80, and 160 corresponding to the D_0 values 0.42, 0.27, and 0.21 Mpc, respectively. We set $V_0 = 350$ km s^{-1}. We analyze the effects of variation in V_0 separately.

Table 1 lists the number of groups $N_{\rm groups}$, the total number of galaxies in groups $N_{\rm gal}$, the median velocity dispersion $\sigma_{v,\rm med}$, and the first and third quartiles of the σ_v distribution for the 6° and 12° slices as well as for the simulation.

The total number of groups with a particular number of members, $N_{\rm mem}$, is more useful than the total number of groups in the catalog as an indicator of the best choice of the D_0 parameter. The decrease in the total number of real groups for very large values of D_0—several groups merge into fewer low-density systems—is balanced by an increase in the number of

TABLE 1

VARIATION OF D_0 ($\delta\rho/\rho$)

Sample	N_{groups}	N_{gal}	σ_{med} (km s^{-1})
	$\delta\rho/\rho = 20$		
Simulation	90	416	242_{157}^{372}
6° slice	81	681	177_{113}^{377}
12° slice	139	1088	177_{109}^{365}
	$\delta\rho/\rho = 80$		
Simulation	41	135	253_{118}^{334}
6° slice	73	501	202_{116}^{271}
12° slice	128	778	196_{111}^{284}
	$\delta\rho/\rho = 160$		
Simulation	17	51	169_{112}^{345}
6° slice	67	421	185_{82}^{295}
12° slice	117	634	171_{97}^{266}

pseudogroups. For very small values of D_0, i.e., high overdensities, the total number of real groups decreases because we exclude many low-density systems from the catalog. However, this decrease is compensated by an increase in the number of groups which are high-density subclumps within the richest systems. The optimal choice of D_0 is a compromise between the need to identify very low density associations of galaxies and the need to minimize the number of pseudogroups in the catalog.

Figures 2*a*, 2*b*, and 2*c* show the cumulative number of galaxies in groups, $N_{gal}(\leq N_{mem})$, with at most N_{mem} members as a function of N_{mem}. For $\delta\rho/\rho = 20$, 80, and 160, the plots compare the 6° slice with the simulation. At $\delta\rho/\rho = 20$ there are more galaxies in pseudogroups with $N_{mem} \leq 10$ than there are in the real groups. At $\delta\rho/\rho = 80$ most of the pseudogroups have $N_{mem} \leq 4$; many of the real groups still have $N_{mem} \geq 4$. At the highest density enhancement the difference between the histograms for the real groups and the pseudogroups is still larger. However, we still find pseudogroups with three members. The list of real groups consists primarily of the cores of the densest groups and of density peaks within the clusters in the survey.

At low $\delta\rho/\rho$, there are many groups in the simulation. Small random fluctuations in the space density with chance alignment nearly along the line of sight produces these pseudogroups. These pseudogroups have properties similar to those of physical groups in the survey. For these pseudogroups, the internal velocity dispersion is dictated by the typical thickness of the structures which surround the voids (~ 500 km s^{-1}). The properties of the pseudogroups are sensitive to the selection parameters.

In contrast, the groups extracted from the redshift survey are stable against variation of $\delta\rho/\rho$. Thirty-four of the groups are stable over the contrast range from $\delta\rho/\rho = 20$ to $\delta\rho/\rho = 80$. Sixty-five groups are stable over the range $\delta\rho/\rho = 80$ to $\delta\rho/\rho = 160$, and 22 over the range $\delta\rho/\rho = 20$ to $\delta\rho/\rho = 160$. In particular, derived parameters of the Coma Cluster are insensitive to the choice of the D_0 parameter. Table 2 is a summary of the properties of the Coma Cluster (velocity dispersion, mass-to-light ratio, and number of members) as a function of $\delta\rho/\rho$.

Following the criterion given at the beginning of this subsection, the comparison of the data with the simulation indicates that $\delta\rho/\rho \simeq 80$ optimizes the identification of physical systems. Results are similar for the 12° slice. Given the coherence of large-scale structure in going from one 6° slice to the adjacent one, the similarity of group catalogs for the 6° and 12° slices is not surprising.

TABLE 2

THE COMA CLUSTER

Density Parameter $\delta\rho/\rho$	N_{mem}	σ_v (km s^{-1})	$M/L_{B(0)}$ ($M_\odot/L_\odot$)
20	182	842	377
80	139	868	357
160	119	900	400

Although the simulated catalog mimics several of the salient features of the data, the group identification algorithm could be sensitive to some of the details of the model. We therefore construct a much simpler model based on a small portion of the data. The data contain a shell (S1) with $14^h30^m \leq \alpha \leq 17^h$, $26\overset{\circ}{.}5 \leq \delta < 32\overset{\circ}{.}5$, and 9200 km s^{-1} $\leq cz \leq$ 10,500 km s^{-1} (see Fig. 1). The sample S1 contains 111 galaxies. This simple structure extending perpendicular to the line of sight is representative of the environment of most galaxies in the survey. It is narrow enough in velocity space that the scaling of the luminosity function is irrelevant to group selection. This model yields a lower limit on the fraction of spurious groups as a function of N_{mem}.

Our simulation of S1 consists of 111 points distributed over the same solid angle and within the velocity range 9200–10,500 km s^{-1}. In an average over 10 simulations, each with 111 randomly distributed points, we find 4 groups with 3 members and 1 group with 4 members. In the data 6 groups have 3 members, 1 has 4, 1 has 5, 2 have 6, and 2 have 10 members. In the data the number of galaxies in rich groups ($N_{mem} \geq 5$) is about a third of the total number of galaxies in groups, approximately the same as the fraction in rich systems over the entire survey.

Many of the groups with 5 or more members are probably real physical systems (see Fig. 2*b*); in other words, they are probably smaller in space than they are in redshift space. Our model of S1 may, therefore, be overly dense. To simulate the effect of this effectively lower background density on group selection, we use 79 randomly distributed galaxies in the simulation of S1. On average, we find 2 groups with 3 members, i.e., about one-third of the number of triples in the data. We find no groups with $N_{mem} > 3$. Taken together, the simulations of S1 suggest that at least a third of the triples in the real group catalog are spurious (although we cannot tell which ones) but that almost all of the $N_{mem} \geq 5$ groups are real.

b) The Selection Parameter V_0 and the Reference Velocity V_f

For each of the data sets in the previous subsection we construct one catalog with $V_0 = 350$ km s^{-1} and one with $V_0 = 600$ km s^{-1} (the first value is close to the one in HG82; the second is the one in GH83). All the catalogs have $D_0 = 0.27$ Mpc ($\delta\rho/\rho = 80$). For each catalog Table 3 lists the number of groups, N_{groups}, the total number of galaxies in groups N_{gal}, the median velocity dispersion $\sigma_{v,med}$, and the first and third quartiles of the σ_v distribution.

Just as for variation of D_0, the catalogs obtained from the data by varying V_0 are much more stable than those obtained

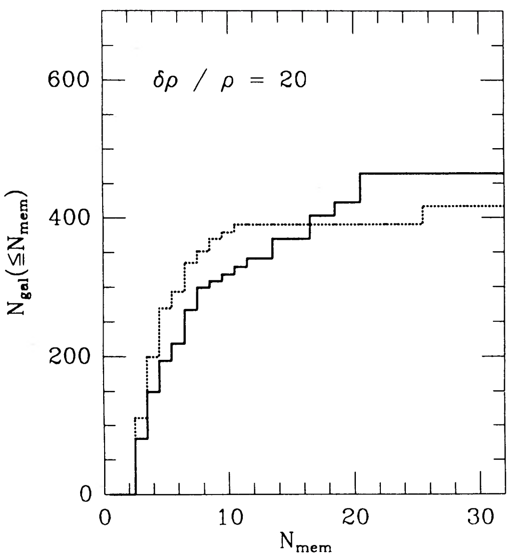

FIG. 2a

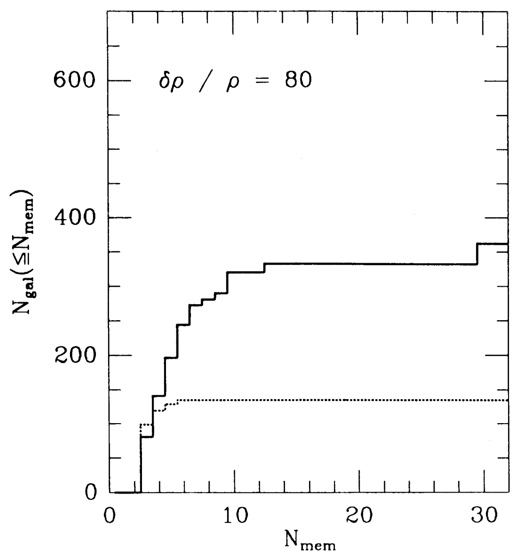

FIG. 2b

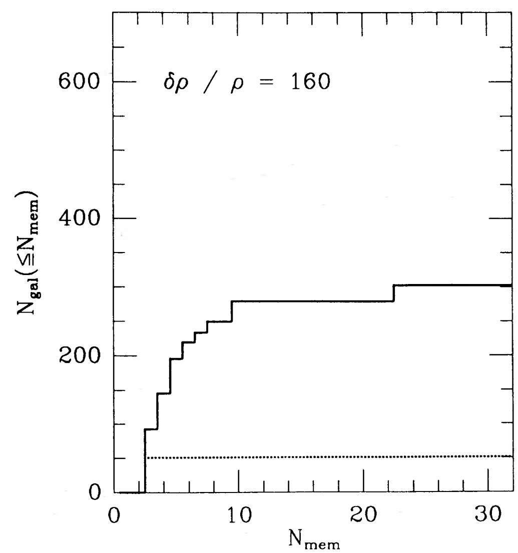

FIG. 2c

FIG. 2.—Cumulative number of galaxies in groups containing at most N_{mem} galaxies as a function of N_{mem}: data (*solid line*) vs. simulation (*dotted line*). The group catalogs have (*a*) $\delta\rho/\rho = 20$, (*b*) $\delta\rho/\rho = 80$, and (*c*) $\delta\rho/\rho = 160$. V_0 is 350 km s^{-1} in all cases.

TABLE 3

VARIATION OF V_0

Sample	N_{groups}	N_{gal}	σ_{med} (km s^{-1})
$V_0 = 350$ km s^{-1}			
Simulation	41	135	253_{118}^{334}
6° slice	73	501	202_{116}^{271}
12° slice	128	778	196_{111}^{284}
$V_0 = 600$ km s^{-1}			
Simulation	57	213	329_{224}^{558}
6° slice	79	549	220_{124}^{475}
12° slice	135	855	220_{122}^{461}

from the simulation. Contamination of the real catalog with pseudogroups is minimized for the smallest reasonable V_0. The lower bound on V_0 is set by the requirement that the velocity dispersions of groups and clusters not be artificially biased toward low values. The scaling of V_0 yields $V_L = 1335$ km s^{-1} at $cz = 10{,}000$ km s^{-1} for $V_0 = 350$ km s^{-1}. This value of V_L is smaller than the typical radii of voids and larger than necessary to avoid biasing the velocity dispersion of the richest clusters. For $V_0 = 600$ km s^{-1}, $V_L = 2288$ km s^{-1}. We now demonstrate that this larger value leads to significant contamination of groups.

Figures 3*a* and 3*b* show the velocity dispersion σ_v as a function of redshift, cz, for all groups in the 12° slice with $V_0 = 350$ km s^{-1} and $V_0 = 600$ km s^{-1}, respectively. Among the systems with $\sigma_v \leq 400$ km s^{-1}, 86/110 ($V_0 = 350$ km s^{-1}) or 86/94 ($V_0 = 600$ km s^{-1}) groups are unaffected by the variation in V_0. Most of the differences between the catalogs are for $\sigma_v \geq 400$ km s^{-1}. In the $V_0 = 350$ km s^{-1} catalog there are 18 groups with $\sigma_v \geq 400$ km s^{-1}; with $V_0 = 600$ km s^{-1} there are 41 of these groups. About half of these groups have fewer than 5 members. Because many groups with a similar range of properties occur in the simulation, a substantial fraction of the groups in the redshift survey are likely to be spurious.

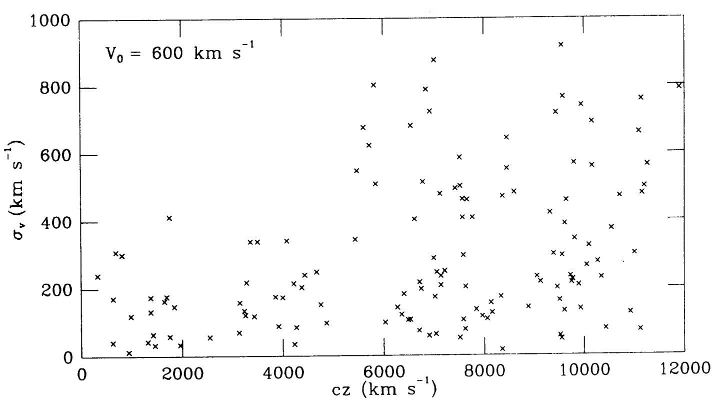

FIG. 3*a*

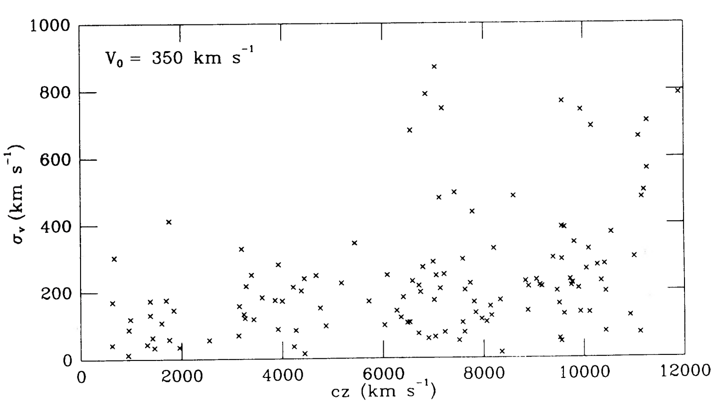

FIG. 3*b*

FIG. 3.—Line-of-sight velocity dispersion, σ_v, as a function of redshift for groups with $\delta\rho/\rho = 80$ and with (*a*) $V_0 = 600$ km s^{-1} (135 groups) and (*b*) $V_0 = 350$ km s^{-1} (128 groups).

At $V_0 = 350$ km s^{-1} the algorithm identifies all seven Abell clusters in the survey. All have $M/L_{B(0)} \leq 1000\ M_\odot/L_\odot$, and the two richest have $\sigma_v \geq 400$ km s^{-1}. The properties of the latter two systems are, in fact, insensitive to the choice of V_0. For $V_0 = 350$ km s^{-1} Coma has 139 members with $\sigma_v = 868$ km s^{-1}, and $M/L_{B(0)} = 357\ M_\odot/L_\odot$; for $V_0 = 600$ km s^{-1}, there are 153 members with $\sigma_v = 875$ km s^{-1} and $M/L_{B(0)} = 376\ M_\odot/L_\odot$. The cluster A1185 does not vary at all. Among all of the groups with $\sigma_v \geq 400$ km s^{-1} in the $V_0 = 600$ km s^{-1} catalog, 27 have $M/L_{B(0)} \geq 1000\ M_\odot/L_\odot$. In the $V_0 = 350$ km s^{-1} catalog, only 10 groups have such suspiciously high mass-to-light ratios.

The selection of $V_0 = 350$ km s^{-1} diminishes the number of high M/L systems in the catalog and preserves most of the richer systems ($N_{\text{mem}} \geq 5$) with $\sigma_v \geq 400$ km s^{-1} and $M/L_{B(0)} \leq 1000\ M_\odot/L_\odot$. With $V_0 = 600$ km s^{-1}, there are 8 of these systems; 7 of them also appear in the $V_0 = 350$ km s^{-1} catalog. Thus, the lower value of V_0 appears to minimize the contribution of contaminated or spurious groups to the set of rich, high velocity dispersion systems in the catalog.

We adopt $V_0 = 350$ km s^{-1} for the final catalog. However, most groups are insensitive to this choice; they are generally more sensitive to the choice of D_0. The insensitivity to the choice of V_0 is probably related to the geometry of large-scale structure. Most of the galaxies in this region are in structures perpendicular to the line of sight. These sheets are generally separated by large voids (with diameters generally larger than V_L). This structure severely restricts the number of interlopers with velocities larger than the ~500 km s^{-1} FWHM of the sheets, provided that V_L remains small compared with the diameters of the voids. As an example of this effect, the shell S1 discussed in the previous subsection yields exactly the same groups for both values of V_0. In this case the foreground void has a diameter of ~5000 km s^{-1}.

We have also examined the sensitivity of the catalog to the choice of the reference velocity, V_f. As in our previous papers (HG82; GH83), we adopt $V_f = 1000$ km s^{-1}. We find that catalogs with $\delta\rho/\rho = 80$ and $V_0 = 350$ km s^{-1} for $V_f = 1000$ km s^{-1} and for $V_f = 3000$ km s^{-1} (note that $\delta\rho/\rho = 80$ for $D_0 = 0.39$ Mpc with $V_f = 3000$ km s^{-1}) have nearly indistinguishable properties.

V. THE GROUP CATALOG

The selection parameters for the group catalog in Table 4 are $D_0 = 0.27$ Mpc ($\delta\rho/\rho = 80$) and $V_0 = 350$ km s^{-1}. Each group has at least three members. The mean velocities of the groups are $\leq 12{,}000$ km s^{-1}, but members may have velocities are large as 15,000 km s^{-1}. In Table 4 each group member is listed with the name assigned in the Center for Astrophysics survey (Huchra *et al.* 1989). The names are related to the right ascension and declination in the usual way.

The catalog includes 128 groups with a total of 778

TABLE 4

Group Catalog

ID		group	members		
1	1044+2633	1044+2648	1045+2651	1046+2702	1047+2700
	1045+2631				
2	N3826	N3830A	N3830B	1142+2702	1142+2707
	1140+2632				
3	1413+2642	1416+2650	I4395	1418+2705	I4399
4	N4849	1255+2707	1254+2710	I 837	N4859
	N4821	N4819	1256+2732	I 835	1255+2708
	1255+2711	1258+2656	1256+2722	1256+2726	N4787
	N4827	I3900	I3913	1254+2744	1258+2740
	N4842	N4839	N4853	N4854	1257+2758
	I3959	N4789	1250+2740	N4798	N4807
	1253+2756	1254+2801	N4816	1253+2805	I3949
	1258+2754	N4926A	1259+2803	N4919	I3976
	1259+2809	N4906	N4911	N4872	N4874
	N4871	1256+2817	N4883	N4860	1255+2824
	I4026	N4926	N4908	I4040	N4895
	1256+2829	I3960	N4876	N4869	N4898W
	N4889	N4864	1257+2819	I4045	1255+2827
	1255+2828	N4848	N4881	1248+2739	1249+2751
	N4788	1300+2807	N4927	I4106E	N4944
	1259+2829	1258+2838	1259+2840	N4841A	N4858
	1259+2857	1255+2859	I4042	N4886	N4929
	I3946	N4850	N4721	1250+2721	1300+2850
	1257+2906	N4841B	1255+2913	1254+2912	1254+2918
	1254+2919	1255+2924	N4931	1259+2822	N4907
	N4896	I4133	N4934	1301+2831	1256+2740
	N4840	N4873	N4828	1255+2749	1247+2710
	N4692	1248+2806	1249+2718	I 842	I4088
	I 843	N4922A	N4922B	N4923	N4921
	1300+2830	N4957	N4892	1256+2755	1257+2808
	1246+2707	1245+2715	1245+2716	N4745	N4715
	I4032	1259+2931	I4051	I3973	N4867
	N4673	1244+2744	N4865	1254+2638	
5	1146+2701	N3900	N3912		
6	I3585	N4556	N4558	I3508	N4555
7	1240+2655	I3618	I3623	I3645	
8	N4670	1242+2845	1244+2650		
9	1212+2710	1213+2717	1213+2743	1213+2656	
10	0916+2708	0916+2740	0914+2756	0917+2658	
11	1217+3010	N4136	N4308	N4150	N4395
	1202+2839	N4245	1202+3108	N4448	N4310
	N4278	N4286	N4274	1229+2959	N4414
	1226+3559	N4163	1212+3630	N4214	N4190
	N4080	N4251	1214+2900	N4173	N4283
	N4314	1218+3104	N4020	1157+3129	N4062
	N4393	N4559	N4509	1230+3753	N4244
	1207+3643	N4359	1219+3222	I3308	
12	1125+2711	1121+2718	1125+2740	1126+2741	1125+2744
	1123+2702				
13	I3376	N4475	I3336		
14	1426+2728	N5635	1428+2727	1427+2745	1426+2729
	I4452	1425+2710			
15	1108+2722	N3570	N3563		
16 *......	1533+2730	1531+2730	1534+2729		
17	N3414	N3418	1046+2811	N3400	N3380
	N3451				
18 *......	1311+2801	N5032	1309+2735		
19	N6269	N6272	N6263	N6264	N6261
	1655+2816	1658+2805	N6265	1659+2830	1658+2740
20 *......	N4016	I2982	N4004A	N4004	N4008
	N4017				
21 *......	1447+2759	1447+2805	I4514		
22 *......	I3593	I3592	I3598	1236+2801	
23 *......	I4572	I4568	I4570	I4569	1538+2831
	I4580	I4581	1541+2835	1541+2841	1539+2809
24 *......	1204+2825	N4104	1201+2826	1204+2813	
25 *......	N4295	I3210	I3263	I3165	
26	N3026	N3032	0947+2815		
27 *......	N4983	N4971	1306+2827	N4966	1305+2858
	1303+2934	1303+2851	1302+2905	1303+2933	1304+2818
28 *......	N3713	1128+2828	N3714	1126+2849	1129+2819
29 *......	1525+2857	I4547	I4546	1525+2901	1524+2901
	1525+2824				
30 *......	1115+2833	1116+2848	1115+2830		
31 *......	N3536	N3539	N3550	N3527	1104+2852
	1104+2859	1108+2900	1107+2900	N3558	N3554
	1108+2858	N3561	1107+2835		
32 *......	1548+2847	N6001	1548+2857	1547+2842	
33 *......	N4185	1209+2905	1210+2907	N4174	N4175
	N4169	N4196			
34 *......	1353+2847	1355+2902	1356+2906	1356+2906	1354+2845
35	N3277	N3245A	N3265	N3254	N3245

1989ApJ...344...57R

TABLE 4—*Continued*

ID			group	members		
36	*......	1217+2907	1217+2909	1217+2900		
37	*......	I4442	N5657	N5641		
38	......	N3486	1102+2925	N3510		
39	*......	1306+2938	I4210	N5004	N5004A	N5000
40	*......	0847+2925	0846+2943	I2404	0848+2923	
41	*......	N4132	N4131	N4134		
42	*......	N6086	1610+2947	1612+2959	1612+3006	N6085
43	*......	1348+2937	I4334	1349+2935		
44	*......	1159+2945	1159+3008	1159+3007	1200+2942	
45	*......	1358+2948	1358+3019	1358+2946		
46	*......	1103+3012	1102+3018	1101+2947		
47	......	N6282 1658+2948	1656+2959	N6274A	1659+3015	1659+3024
48	*......	I2476	I2479	0926+3022	I2473	I2480
49	*......	N2783	N2783B	0911+3020	I2444	N2789
50	*......	N5277 1340+3036	N5282 1338+3038	N5271 N5280	1340+3030	1342+3035
51	*......	N5642	1426+3018	1425+3010		
52	*......	1650+3048	1650+3048	1651+3035		
53	*......	1426+3051 1424+3145	1429+3100 N5639A	I1012	I4447	N5653
54	*......	1519+3050	1519+3050	1518+3039		
55	*......	I2985	I2986	1154+3040		
56	*......	1436+3101	1436+3110	1435+3042		
57	*......	1314+3056 N5074	N5056 1312+3045	N5057	1315+3118	N5065
58	*......	1316+3102	1316+3107	1318+3051	1314+3047	
59	......	N5961	1532+3114	1534+3051		
60	*......	I4256	N5187	1327+3139	1328+3153	1326+3105
61	*......	1317+3115	1319+3130	1319+3139	1319+3148	1317+3110
62	*......	1615+3119	1613+3131	1613+3112		
63	*......	1202+3126 1203+3120	1202+3127	I3007	1206+3151	1208+3156
64	*......	1520+3124	1517+3133	N5924		
65	*......	1319+3137 1320+3205	1318+3147 I4225	1321+3136 I4226	N5127 1318+3129	1321+3154
66	*......	1337+3134	1336+3138	1336+3131		
67	*......	N5025	1309+3146	1308+3143	1310+3131	
68	......	1140+3144	1140+3145	1139+3217	1143+3135	
69	*......	0933+3202	0931+3217	N2918		
70	......	0939+3205	N2968	N2970	N2964	
71	*......	1158+3209	N4031	1157+3205		
72	*......	1234+3221	1235+3222	1234+3223	1236+3216	
73	*......	N3986 N3991	1154+3225 1154+3253	N3966 I2978	N3994	N3995
74	*......	1006+3245	1003+3229	1007+3219		
75	*......	N2944	0936+3236	0936+3236	0938+3223	
76	......	N4631	N4627	1242+3440	1244+3645	N4656
77	......	0945+3307 N3067 N3011	0948+3310 I2524	N3003 0958+3322	N3021 1003+3311	0952+3330 N3118
78	*......	1624+3252	N6162	N6163	1623+3235	
79	*......	I2439	0908+3302	0906+3243		
80	*......	1131+3327	1130+3346	1131+3254		
81	*......	I3003	N4122	I2993	1206+3256	
82	*......	N3871 I2953	N3881 N3847	N3880 1141+3256	N3878	I 729
83	......	N3424 1050+3417	N3430 1049+3445	N3395 N3381	N3396 I2604	N3442
84	*......	0918+3337	N2832	0920+3358	0919+3403	0917+3317
85	*......	N5098A	N5098A	1318+3333	1318+3336	N5096
86	*......	1638+3346	1639+3352	1639+3327		
87	*......	I4496	I4505	I4506		
88	*......	N5321	N5318	N5312		
89	*......	0930+3408	0931+3413	0932+3413	0930+3416	0930+3353
90	*......	1135+3408	1136+3413	1138+3357		
91	*......	1119+3436 I2744	1120+3437 I2738	1117+3422 1120+3406	1116+3424	I2735
92	*......	1344+3408	1345+3424	1344+3407		
93	*......	1617+3440	1619+3453	1621+3507	1617+3427	
94	......	1312+3509 N5002	I4213 N5005	1311+3629 1307+3427	N5014	N5033
95	......	N2780	N2778	0909+3544	N2793	
96	*......	1211+3454	1210+3459	1212+3453		

TABLE 4—*Continued*

ID		group	members		
97 *......	0942+3455	0944+3500	0941+3455		
98 *......	N5228	1333+3515	N5223	1334+3500	N5233
99 *......	1400+3506 1401+3559	N5445 N5440	N5444	N5399	1402+3547
100 *......	N6109	N6116	N6107		
1C1	1138+3529 N3694A	1135+3528 N3813	1133+3536 1122+3554	1129+3536 1143+3508	N3755
102 *......	0934+3526	0934+3549	0932+3513		
103 *......	1151+3526	1148+3529	N3897	1150+3518	
104 *......	N4956	N4986	1304+3522		
105 *......	N5590	N5589	1422+3529	N5579	
106 *......	1123+3537 1124+3531	1123+3542	1122+3547	N3695	1124+3619
107 *......	1621+3557 1620+3546	1619+3610	1622+3620	1617+3612	N6126
108 *......	1404+3601	N5499	1402+3602	N5517	1406+3551
109 *......	1646+3559	1646+3601	1647+3618	1644+3610	1646+3555
110 *......	N2719A	N2724	N2719		
111 *......	1609+3605	1609+3607	1607+3555		
112 *......	N6199 1635+3633	I4614 1633+3556	N6197	N6194	1635+3631
113 *......	0909+3608	0911+3617	0911+3618	0909+3559	
114 *......	1137+3624	1137+3657	1136+3602		
115 *......	N2965 N2955	I2500	0942+3623	N2971	0942+3645
116 *......	N5149 1322+3610	N5141	N5142	N5143	1322+3651
117 *......	I4028	I4049	1256+3611		
118 *......	0847+3630 0846+3617	0847+3639	N2668	0845+3657	I2405
119 *......	1117+3622	1114+3625	1112+3647	1114+3620	
120 *......	N5557	N5544	N5545	N5529	
121 *......	N5684	N5695	1433+3656	1433+3701	N5686
122 *......	N3542	1107+3716	1109+3700		
123	N3930	1155+3821	N3941		
124	0904+3742 0906+3814	0905+3742 0909+3752	N2759 I2434	I 527	0906+3754
125	N6137 N6120	1620+3804 N6119	1621+3804 1618+3821	N6129 1621+3740	1620+3829
126	N5394 N5395	N5380	N5378	N5403	1357+3826
127	N5351	1349+3819	1351+3828	N5341	
128	1102+3820	1101+3828	1102+3817		

NOTE.—An asterisk denotes a group belonging to the statistical sample of 92 groups used in the analysis of group properties.

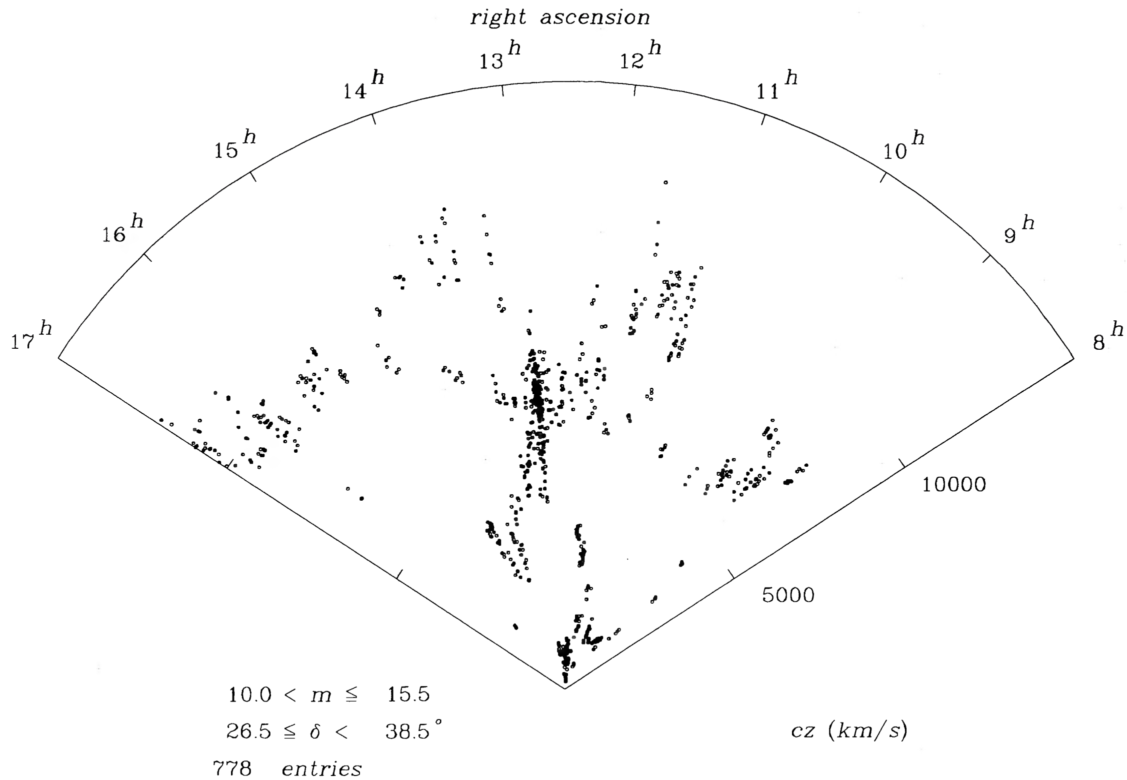

FIG. 4a

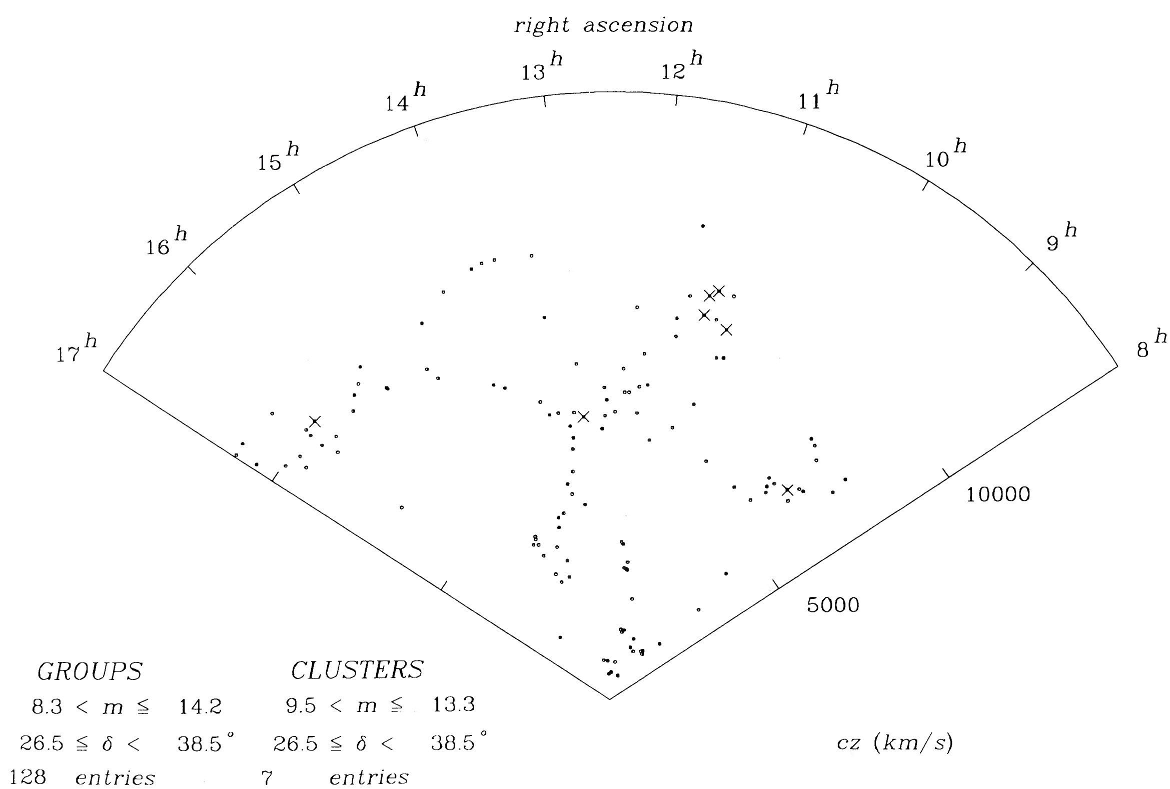

FIG. 4b

FIG. 4.—(a) Cone diagram for group members in the declination range $26^\circ.5 \leq \delta < 38^\circ.5$. There are 778 galaxies. (b) Cone diagram for groups; each point represents one of the 128 groups in the catalog with mean redshift $cz \leq 12{,}000$ km s^{-1}. The crosses indicate the locations of Abell clusters. Compare Fig. 1.

members. The algorithm also identifies 142 binaries (not included in this analysis). The number of galaxies not assigned to a group or binary is 614. The sum of these numbers is not equal to the total number of galaxies in the survey (1766) because galaxies with velocities greater than 12,000 km s^{-1} are considered only if they are contained in groups with mean velocity less than 12,000 km s^{-1}.

Figures 4*a* and 4*b* are cone diagrams which show the distribution of group members and group centers, respectively. Comparison of Figure 4*b* with Figure 1 shows that the group centers mark the large-scale structure in a nearly unbiased way. More detailed comparison of Figures 4*a*–4*b* with Figure 1 shows that projection effects in Figure 1 can hide "fingers" as well as produce misleadingly impressive ones. These impressions are a result of averaging over an angular scale which is large compared with a typical group diameter.

VI. GROUP PROPERTIES

Here we examine the typical physical properties of the groups in the catalog. We first trim the catalog by eliminating groups which may have properties affected by the proximity of the sample limits. We include only groups with velocities > 2000 km s^{-1}. At smaller distances the declination angle spanned by the survey is smaller than or at best comparable to the angular scale of a typical group. We also discard groups with baricenters closer to the edges of the survey than $2R_p$. This criterion deletes the Coma Cluster from our "statistical sample" of groups. Asterisks in Table 4 mark the groups in the statistical sample.

a) *Physical Properties*

Table 5 lists the properties of the 92 groups in the "statistical sample." For each group, we list the group number (col. [1]), the number of members (col. [2]), the right ascension (col. [3]), the declination (col. [4]), the mean velocity (col. [5]), the rms line-of-sight velocity dispersion σ_v (col. [6]), the apparent magnitude corresponding to the sum of the apparent luminosities of the observed group members (col. [7]), the mean pairwise separation R_p (col. [8]), the mean harmonic radius R_h (col. [9]), the crossing time t_c in units of $t_0 = H_0^{-1}$ (col. [10]), the logarithm of the virial mass, log M (col. [11]), and the mass-to-light ratio, $M/L_{B(0)}$ (col. [12]). These quantities are also available for groups in the catalog of HG82. Table 6 gives medians for the distributions of σ_v, log M, M/L, T_c, R_h, and R_p. We also include the first and third quartiles for these distributions.

The quantities in Table 5 and 6 are number-weighted. Weighting with luminosity in the calculation of group parameters does not significantly affect the median quantities in Table 6 (see Heisler, Tremaine, and Bahcall 1985). The median mass-to-light ratio and crossing time do not change at all. Figure 5 shows the logarithm of the unweighted $M/L_{B(0)}$ as a function of the logarithm of the luminosity-weighted value. The scatter around the mean relation is remarkably small.

We next consider the properties of groups with $N_{\rm mem} \geq 5$. These groups are statistically the most reliable; at least 33% of groups with $N_{\rm mem} < 5$ are spurious (see § IV). Table 6 gives the median values and quartiles for the physical parameters of the 36 groups with $N_{\rm mem} \geq 5$.

Figures 6*a*–6*f* are histograms of the distribution of σ_v, R_h, R_p, t_c, log $(M/L_{B(0)})$, and log M, respectively. The unfilled histograms refer to the entire sample of 92 groups; the hatched histograms refer to the 36 groups with $N_{\rm mem} \geq 5$. There are no salient differences between the distributions for the groups with $N_{\rm mem} \geq 5$ and the full sample. Because the properties of contaminated and/or spurious groups containing three or four members are statistically indistinguishable from those of real physical systems, we cannot remove pseudogroups from the sample. However, the median values obtained for the whole sample appear to be a fair representation of the properties of real groups.

The spread of mass-to-light ratios as measured by the quartile range is similar to the spread obtained for other catalogs (Rood and Dickel 1978; Tully 1987; Huchra and Geller 1982). We obtain a spread of 0.9 in the logarithm of $M/L_{B(0)}$ as measured by the range between the first and third quartiles. This spread is somewhat larger than the statistical spread (~0.7) obtained by Heisler, Tremaine, and Bahcall (1985) for systems with fixed mass-to-light ratio. The significance of the difference

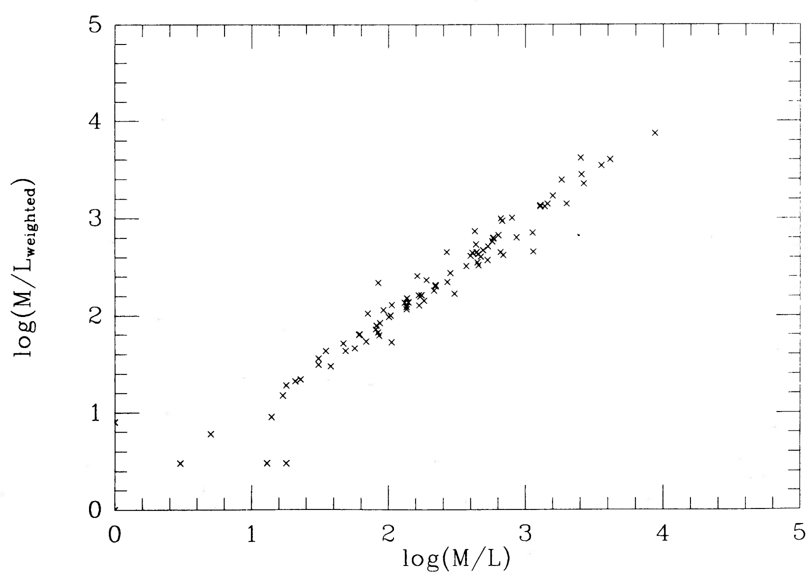

FIG. 5.—Logarithm of the luminosity-weighted mass-to-light ratio as a function of the logarithm of the unweighted value. We include only the 92 groups in the statistical sample (Table 5).

TABLE 5

GROUP PROPERTIES

ID	N_{mem}	α_{1950}	δ_{1950}	cz ($km\ s^{-1}$)	σ_v ($km\ s^{-1}$)	m_{tot}	R_p (Mpc)	R_h (Mpc)	t_c/t_0	$log\ M/M_\odot$	$M/L_{B(0)}$ ($M_\odot/L_\odot$)
1	6	8 46.4	36 46	7515.	51.	13.00	0.96	0.93	0.98	12.53	23.
2	4	8 46.9	29 32	7958.	115.	13.90	0.77	0.37	0.17	12.83	87.
3	3	8 57.4	35 55	3130.	69.	13.40	0.08	0.00	0.00	9.68	1.
5	3	9 6.8	32 50	4235.	35.	13.90	0.45	0.42	0.64	11.86	69.
7	4	9 10.5	36 10	6991.	287.	13.70	0.51	0.30	0.06	13.53	573.
8	5	9 10.9	30 12	6586.	229.	12.60	0.50	0.29	0.07	13.33	163.
10	5	9 18.6	33 46	6786.	270.	12.60	0.89	0.99	0.20	14.00	689.
11	5	9 25.2	30 16	8057.	107.	13.30	0.69	0.53	0.27	12.93	57.
12	5	9 30.9	34 8	8129.	154.	13.50	0.54	0.55	0.19	13.26	140.
13	3	9 32.7	32 5	6703.	73.	13.20	0.52	0.54	0.40	12.60	49.
14	3	9 33.8	35 29	6405.	181.	14.10	0.76	0.88	0.26	13.60	1280.
15	4	9 36.9	32 31	6535.	106.	13.40	0.36	0.00	0.00	10.67	1.
17	6	9 40.5	36 27	6745.	196.	12.60	0.74	0.70	0.19	13.57	266.
18	3	9 42.7	34 56	6035.	98.	13.80	0.59	0.66	0.36	12.95	270.
21	3	10 5.7	32 30	6084.	248.	13.90	0.78	0.94	0.20	13.91	2661.
28	3	11 2.5	30 5	8894.	212.	13.90	0.88	0.99	0.25	13.79	491.
29	13	11 7.0	28 53	9576.	765.	12.30	1.00	0.58	0.04	14.67	581.
30	3	11 7.8	37 9	8838.	228.	14.10	0.61	0.32	0.07	13.36	221.
32	4	11 14.8	36 28	7579.	105.	13.60	0.91	0.77	0.39	13.07	136.
33	3	11 15.7	28 37	9745.	215.	13.80	0.45	0.30	0.07	13.28	86.
34	8	11 18.8	34 29	10433.	196.	13.10	0.96	0.69	0.19	13.57	61.
35	6	11 24.3	35 47	10269.	275.	13.20	1.12	0.90	0.18	13.98	190.
37	5	11 28.6	28 31	6902.	58.	12.90	0.60	0.51	0.47	12.37	21.
38	3	11 31.2	33 22	2553.	56.	13.70	0.34	0.38	0.37	12.21	436.
40	3	11 36.9	34 6	10156.	691.	14.00	0.83	0.81	0.06	14.73	2567.
41	3	11 37.3	36 27	11901.	789.	14.20	1.83	2.08	0.07	15.26	4142.
44	8	11 42.8	33 27	9558.	293.	12.90	0.84	0.51	0.09	13.78	132.
46	4	11 49.2	35 22	6486.	105.	13.30	0.81	0.74	0.38	13.06	175.
48	8	11 54.3	32 30	3236.	133.	11.80	0.22	0.17	0.07	12.62	106.
49	6	11 55.6	28 4	3433.	117.	12.20	0.26	0.13	0.06	12.40	84.
50	3	11 56.1	30 55	3262.	121.	13.70	0.35	0.27	0.12	12.74	799.
51	3	11 57.9	32 9	7835.	135.	13.90	0.20	0.24	0.10	12.79	84.
52	4	12 0.0	29 55	3284.	217.	13.20	0.25	0.18	0.05	13.08	1130.
53	4	12 3.4	28 22	8598.	483.	13.10	0.70	0.36	0.04	14.07	531.
54	6	12 4.6	31 36	7124.	479.	12.80	1.14	0.38	0.04	14.09	863.
55	4	12 4.9	33 6	7775.	436.	13.70	0.65	0.68	0.08	14.26	1995.
56	3	12 6.4	29 31	3861.	175.	12.90	0.09	0.10	0.03	12.65	215.
57	7	12 10.4	29 8	3915.	87.	11.70	0.38	0.21	0.13	12.36	35.
58	3	12 11.5	34 55	9727.	233.	14.20	0.75	0.78	0.18	13.77	399.
61	3	12 17.2	29 5	7617.	76.	14.20	0.16	0.11	0.08	11.94	17.
62	4	12 19.3	28 28	8201.	325.	13.60	0.97	1.06	0.17	14.19	1281.
65	4	12 35.0	32 20	7038.	62.	13.60	0.46	0.37	0.32	12.30	31.
66	4	12 35.1	28 10	7730.	222.	13.80	0.73	0.62	0.15	13.63	533.
71	3	12 57.7	36 26	8360.	15.	14.20	0.67	0.60	0.98	11.96	13.
72	3	13 4.4	35 25	4871.	97.	12.80	0.49	0.55	0.31	12.86	171.
73	10	13 4.4	28 56	7174.	746.	12.40	1.09	1.00	0.07	14.89	3571.
74	5	13 8.0	29 42	6550.	681.	12.90	0.66	0.38	0.03	14.39	2531.
75	4	13 9.6	31 46	6849.	788.	13.30	0.71	0.80	0.05	14.84	8758.
77	3	13 10.6	27 53	6278.	141.	13.20	0.53	0.22	0.08	12.78	92.
78	7	13 14.3	31 13	5724.	170.	12.40	0.65	0.46	0.14	13.26	183.
79	4	13 16.5	30 56	9608.	130.	13.90	0.90	0.83	0.34	13.29	104.
80	5	13 18.1	33 27	11163.	478.	13.40	0.40	0.26	0.03	13.91	136.
81	5	13 18.6	31 28	7224.	76.	13.40	0.63	0.51	0.36	12.62	47.
82	9	13 19.7	31 51	5179.	225.	12.50	0.67	0.54	0.13	13.58	586.
83	6	13 22.7	36 32	5441.	344.	12.40	0.46	0.24	0.04	13.60	454.
84	5	13 26.9	31 26	7213.	249.	13.10	0.91	0.90	0.19	13.89	659.
85	5	13 33.0	35 2	7582.	294.	12.90	0.51	0.49	0.09	13.77	371.
86	3	13 36.7	31 34	4755.	151.	14.00	0.16	0.19	0.07	12.78	440.
87	8	13 40.5	30 25	11266.	706.	12.90	0.97	0.98	0.04	14.83	635.
88	3	13 44.9	34 12	4675.	248.	13.70	0.20	0.09	0.02	12.87	427.
89	3	13 48.1	33 54	4442.	238.	13.10	0.14	0.15	0.03	13.07	448.
90	3	13 48.4	29 42	11269.	564.	14.20	0.97	1.09	0.10	14.68	1452.
92	5	13 55.2	28 57	11209.	499.	13.60	0.92	0.01	0.00	12.47	5.
94	3	13 58.7	29 57	8158.	125.	14.00	0.67	0.23	0.10	12.71	62.
95	7	14 0.7	35 21	4002.	172.	11.90	0.57	0.44	0.14	13.26	304.
96	5	14 6.5	35 59	8328.	172.	13.30	1.68	1.65	0.52	13.83	411.
97	4	14 15.0	36 41	3151.	157.	11.70	0.25	0.00	0.00	10.69	1.
99	4	14 19.9	35 27	3387.	250.	12.80	0.34	0.22	0.05	13.28	1142.
100	3	14 26.4	30 14	4446.	14.	13.70	0.28	0.16	0.24	11.41	18.
101	7	14 26.7	31 7	3927.	281.	12.40	0.58	0.59	0.11	13.81	1838.
102	3	14 27.4	29 13	4222.	213.	12.60	0.36	0.38	0.09	13.37	676.
104	5	14 34.1	36 50	4276.	84.	12.90	0.24	0.21	0.13	12.31	71.
105	3	14 36.4	30 57	10439.	77.	14.20	0.84	0.78	0.55	12.81	31.
106	3	14 43.7	33 36	9053.	232.	14.00	0.76	0.18	0.04	13.14	106.
107	3	14 47.7	27 56	9382.	298.	14.10	0.68	0.55	0.10	13.83	473.
108	3	15 18.9	30 46	9503.	161.	13.80	0.32	0.20	0.07	12.86	38.
109	3	15 19.2	31 27	9553.	47.	13.80	0.70	0.17	0.20	11.72	3.
110	6	15 25.2	28 53	10346.	228.	12.80	0.59	0.14	0.03	12.99	14.
111	3	15 33.0	27 29	10052.	264.	14.20	0.73	0.81	0.16	13.89	453.
113	10	15 40.0	28 26	9891.	206.	12.70	0.99	0.84	0.22	13.70	82.
114	4	15 47.5	28 48	9615.	388.	13.50	0.81	0.79	0.11	14.22	660.
115	3	16 8.6	36 2	9458.	198.	14.20	0.68	0.40	0.11	13.33	167.
116	5	16 11.2	29 47	10093.	323.	13.30	0.90	0.76	0.13	14.04	283.
117	3	16 14.1	31 20	7056.	245.	14.10	0.69	0.82	0.18	13.84	1585.
118	3	16 16.1	35 8	9159.	212.	13.70	0.58	0.58	0.15	13.56	221.
119	4	16 19.1	34 46	10107.	134.	13.80	1.44	1.37	0.55	13.53	137.
121	6	16 20.1	36 9	9933.	136.	13.20	1.21	1.31	0.51	13.53	81.
122	4	16 25.2	32 50	11006.	299.	13.90	1.18	0.32	0.06	13.60	101.
123	7	16 35.3	36 15	9807.	344.	12.80	0.80	0.53	0.08	13.94	168.
124	3	16 39.0	33 41	9518.	57.	14.00	0.68	0.70	0.66	12.49	18.
125	5	16 46.4	36 4	9945.	740.	13.60	0.68	0.52	0.04	14.60	1383.
126	3	16 50.7	30 43	11123.	73.	14.00	0.40	0.00	0.00	10.27	0.

TABLE 6

MEDIAN VALUES OF PHYSICAL PARAMETERS

Parameter	Median	1st Quartile	3d Quartile
All Groups, $N_{groups} = 92$			
σ_v (km s^{-1})	209	111	290
$\log(M/M_\odot)$	13.30	12.72	13.84
$M/L_{B(0)}$ $(M_\odot/L_\odot)$	186	70	583
t_c/t_0	0.06	0.03	0.10
R_h (Mpc)	0.51	0.23	0.78
R_p (Mpc)	0.67	0.45	0.84
Rich Groups, $N_{groups} = 36$			
σ_v (km s^{-1})	228	145	344
$\log(M/M_\odot)$	13.59	12.96	13.96
$M/L_{B(0)}$ $(M_\odot/L_\odot)$	175	76	583
t_c/t_0	0.06	0.03	0.10
R_h (Mpc)	0.52	0.34	0.80
R_p (Mpc)	0.69	0.56	0.96

between the spread in our catalog and the spread obtained for simulations (Heisler, Tremaine, and Bahcall 1985) is probably not significant. It is thus reasonable to conclude that the intrinsic scatter in mass-to-light ratio is small.

b) Distance Dependence of Group Properties

Distance dependence of group properties is one indication of selection bias in a group finding algorithm. Here we examine the 92 group sample for distance dependence.

Figure 7 shows V_L (*dashed curve*) along with the median σ_v (*filled circles*) as a function of redshift. For each redshift bin, the vertical bars span the range from the first to the third quartile of the σ_v distribution. The median velocity dispersion of groups is far from any limit imposed by the selection parameter and is nearly independent of redshift.

Figures 8*a*–8*d* shows σ_v, log $(M/L_{B(0)})$, log t_c, and R_h as a function of the mean redshift of the group. Figure 8*d* shows a clear increase in the envelope of R_h with redshift; we identify the largest groups only at the largest distances. However, there are also many small groups at these distances. In contrast, the simulated catalog contains only large groups at large distances. No strong distance-dependent effects are present for σ_v (Fig. 8*a*) or for log $(M/L_{B(0)})$ (Fig. 8*b*). The crossing time (Fig. 8*c*) is also distance-independent; a bias here would be surprising because the algorithm is designed to keep time scales distance-independent.

c) Groups and Abell Clusters

There are seven Abell clusters in the region of redshift space covered by the survey: the algorithm identifies all seven. Table 7 includes the group number, the richness class, the number of members (two values) σ_v (two values), and $M/L_{B(0)}$ for each of the clusters. The first values of N_{mem} and σ_v come from this analysis; the second values come from Zabludoff, Huchra, and Geller (1989) and typically include velocities for galaxies fainter than those in the redshift survey sample. Other properties for these clusters (except Coma) are in Table 5. Considering the differences in sampling, the velocity dispersions we obtain for A1185, A1228, A1267, and Coma are in reasonable agreement with those from Zabludoff *et al.*

For A1257 and A779, the values of σ_v obtained here are substantially smaller than those obtained by Zabludoff, Huchra, and Geller (1989). In both cases the exclusion of a small number of members (one of the two additional members in A1257 and three of the 15 additional members in A779) in the larger Zabludoff *et al.* samples brings the dispersions into agreement. The sensitivity of the dispersion to the details of the membership assignment underscores the need to obtain complete, magnitude-limited samples for reliable determination of cluster velocity dispersions. Only with such controlled sampling can objective methods for membership selection be applied. In the analysis below, we take the values from this analysis; we thus preserve the uniformity of the selection criteria over the entire catalog.

Arrows above the histograms in Figures 6*a*–6*f* mark the values we obtain for σ_v, $M/L_{B(0)}$, M, T_c, R_h, and R_p for the seven Abell clusters in the sample. In the $M/L_{B(0)}$ histogram the values for the Abell clusters straddle the peak of the distribution; the median $M/L_{B(0)}$ for these clusters is similar to the one for all of the groups in the catalog. For the other quantities (except t_c) the medians for the clusters are larger than those for the catalog as a whole.

The substantial overlap in the properties of groups and Abell clusters suggests that the distinction between groups and clusters is artificial. The survey includes a continuum of systems. In fact there are many groups which share the characteristics of the Abell clusters and some which appear to be even more "cluster-like" than systems included by Abell. Abell does claim that his selection is biased for velocities $\lesssim 6000$ km s^{-1}; however, most of the systems we identify are at velocities $\gtrsim 6000$ km s^{-1} (see § VI*e*). Possible explanations for the apparent discrepancies in the identification of rich systems include (1) incompleteness in the Abell catalog, (2) biases in the selec-

TABLE 7

ABELL CLUSTERS

Abell Cluster	Group Number	Abell Richness Class	N_{mem} [a]	σ_v [a] (km s^{-1})	$M/L_{B(0)}$ [a] $(M_\odot/L_\odot)$	N_{mem} [b]	σ_v [b] (km s^{-1})
Coma	70	2	139	868	357	234	1016
A1185	29	1	13	765	581	16	873
A1228	34	1	8	196	61	8	188
A779	10	0	5	270	689	20	627
A1257	35	0	6	275	190	8	470
A1267	36	0	6	223	169	6	217
A2162	116	0	5	323	283	…	…

[a] This paper.
[b] Zabludoff, Huchra, and Geller 1989.

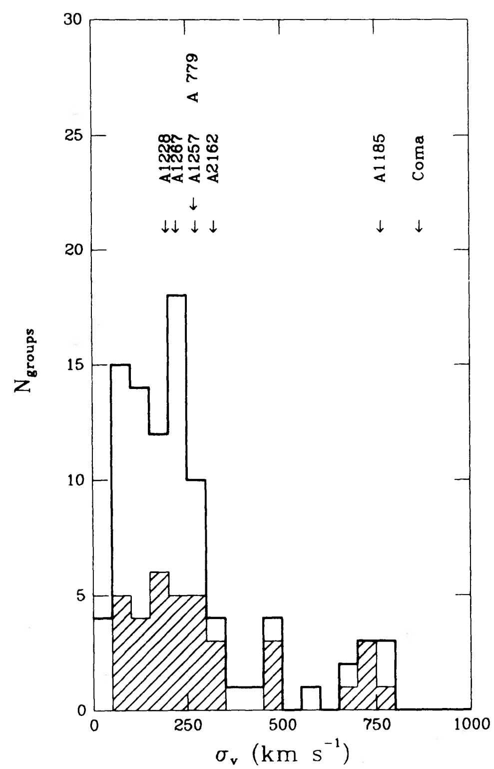

FIG. 6a

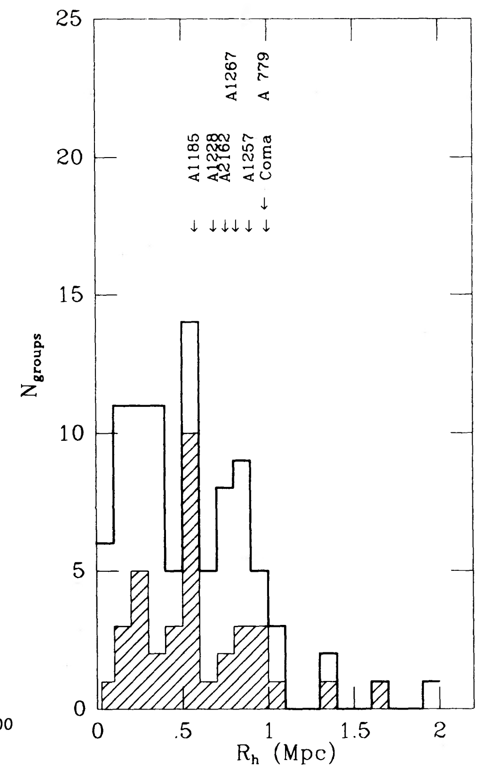

FIG. 6b

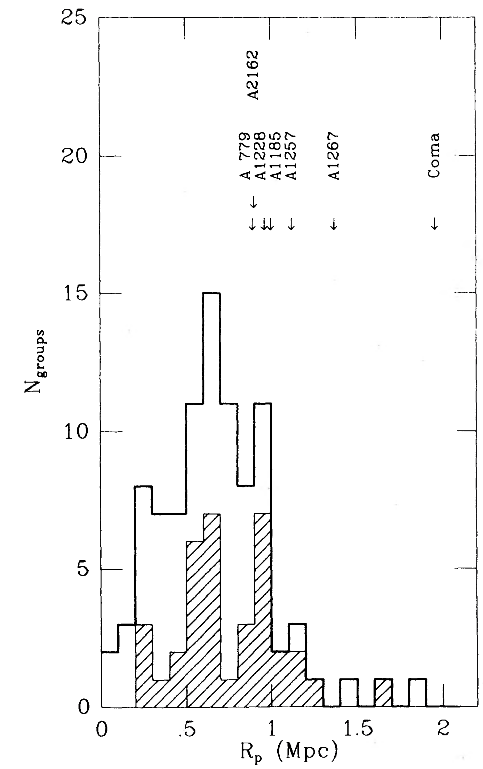

FIG. 6c

FIG. 6.—Histograms of physical properties of groups. The hatched areas refer to the subsample of 36 groups with $N_{mem} \geq 5$. (*a*) σ_v, (*b*) R_h, (*c*) R_p, (*d*) t_c/t_0, (*e*) $\log(M/L_{B(0)})$, (*f*) $\log M$.

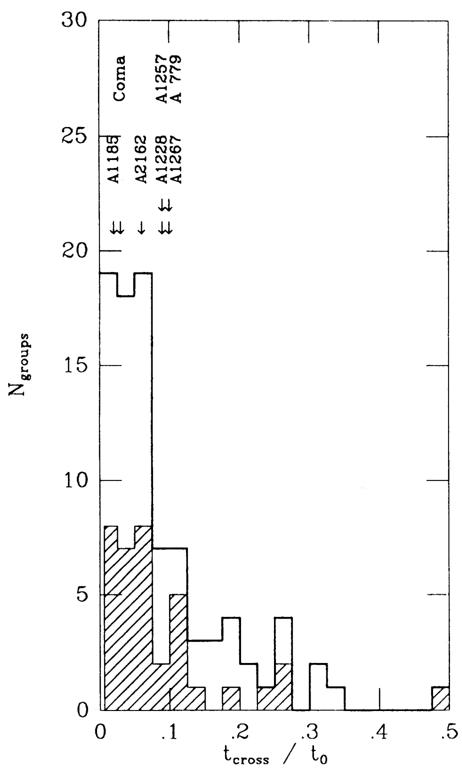

FIG. 6d

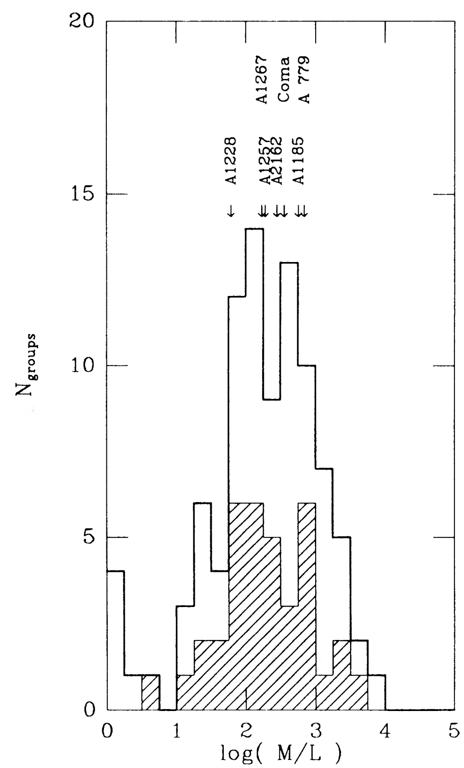

FIG. 6e

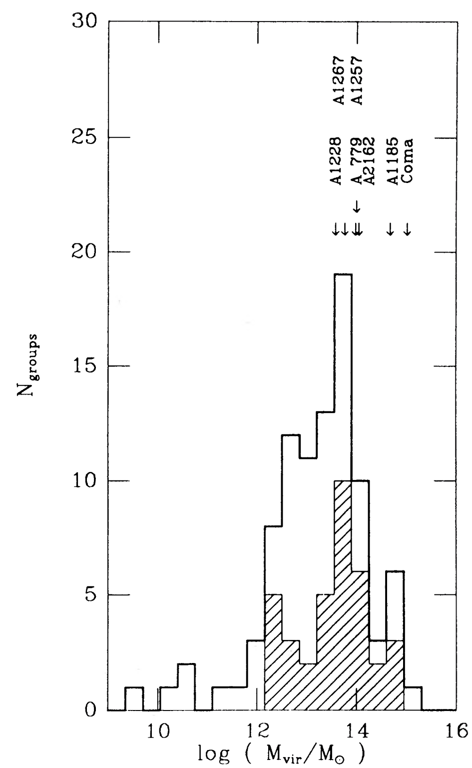

FIG. 6f

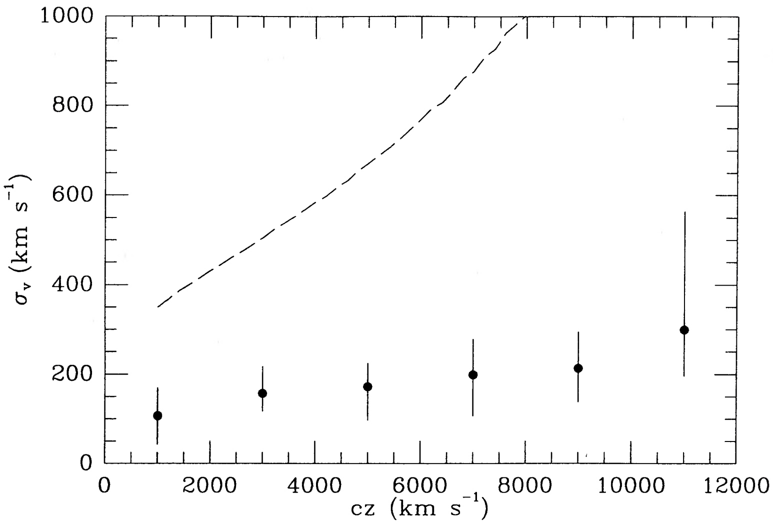

FIG. 7.—Selection parameter V_L (*dashed line*) and the median σ_v (*filled circles*) as a function of redshift. The bars span the range from the first to the third quartile.

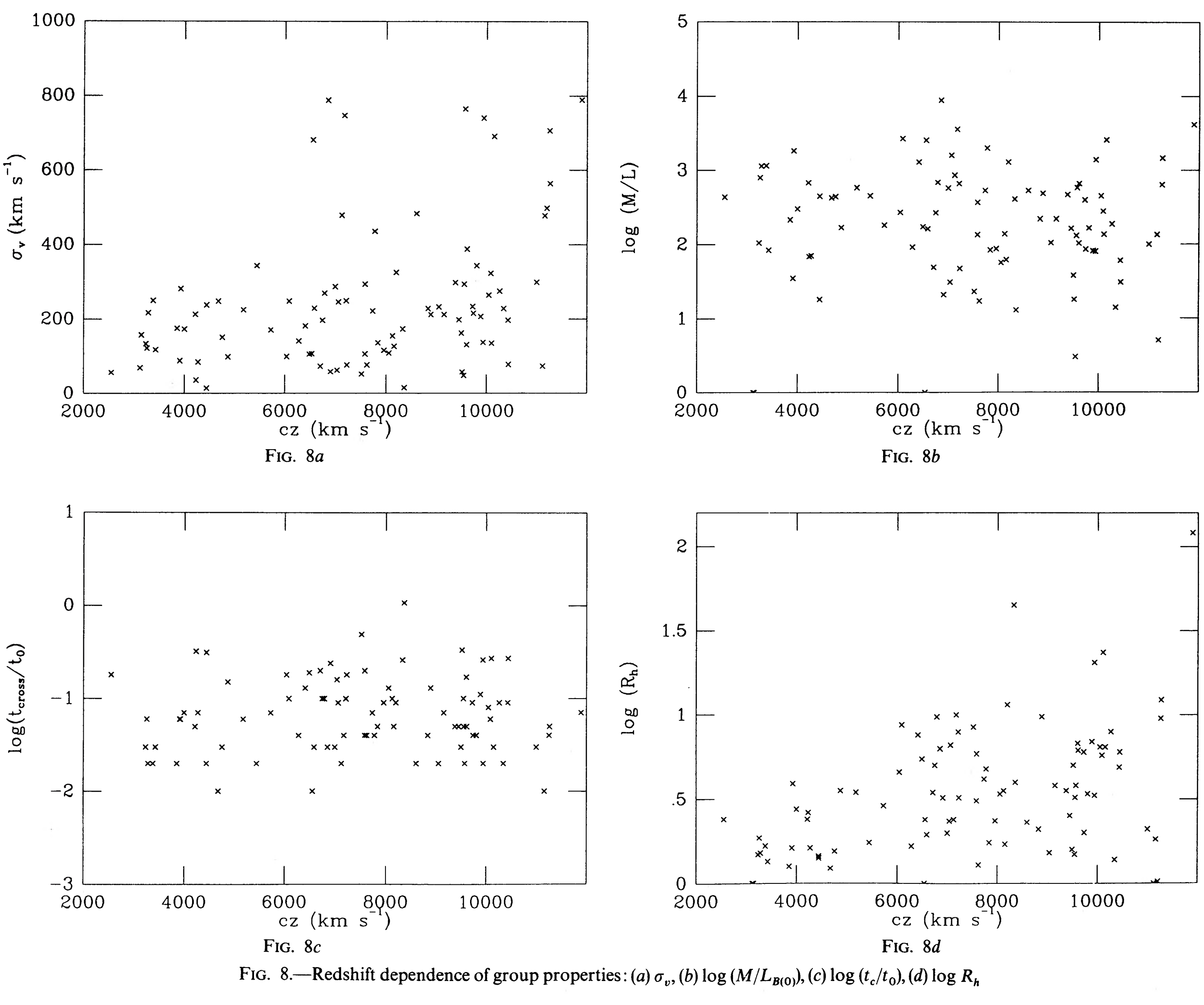

FIG. 8.—Redshift dependence of group properties: (*a*) σ_v, (*b*) log $(M/L_{B(0)})$, (*c*) log (t_c/t_0), (*d*) log R_h

tion of clusters from the distribution of galaxies on the sky rather than from a redshift survey, (3) differences in the morphological composition of Abell clusters and "groups" (in the sense that the Abell clusters are richer in early-type galaxies), and (4) differences in the luminosity function for galaxies in groups and clusters. Some of these issues may be important for attempts to understand the relationship between the correlation function for rich clusters and the correlation function for the galaxy distribution.

d) Groups and Large-Scale Structure

The cone diagram in Figure 4*b* shows the position of all of the groups in the survey, including those which lie near the survey limits. The crosses mark the positions of Abell clusters. The groups trace out the large-scale structure evident in Figure 1. At first glance, the groups appear to be nearly uniformly distributed within the sheets (we will soon report a more detailed analysis of the distribution of groups; Ramella, Geller, and Huchra 1989).

e) Comparison with Other Group Catalogs

Previous complete group catalogs (Tully 1987; HG82; GH83) are generally shallower than the catalog derived from this survey. The region of overlap between this and other catalogs is, thus, small. In order to make a comparison with groups identified in other complete redshift surveys, we applied the search algorithm once again to the original CfA survey with $m_{B(0)} \leq 14.5$ (Huchra *et al.* 1989). The group selection parameters and the luminosity function parameters are the ones used to produce the catalog discussed in § V (Table 4) and differ from those in GH83. Here we take a 300 km s^{-1} Virgo infall into account.

For the 124 groups in the $m_{B(0)} \leq 14.5$ catalog, the median velocity dispersion is $\sigma_v = 131$ km s^{-1} and the median $M/L_{B(0)}$ is 250. These results agree very well with those obtained by NW. NW argue correctly that the V_0 used by GH83 is too large; it is so large that groups include members on both the near and far edges of a void. On the other hand, the difference between the scaling in equation (4) and the scaling used by NW does not affect the results. In both cases the steps in velocity are small enough to avoid the problem in GH83.

The median velocity dispersions differ by about the quartile range for the 14.5 and 15.5 (Table 6) group catalogs. However, the median mass-to-light ratios are well within the quartile ranges. A natural first reaction is that the difference in velocity dispersion is an artifact introduced by the group identification algorithm. We now demonstrate that the difference in the physical parameters of the groups in the two samples is a physical effect related to the properties of large-scale structure. Tully (1987) has previously suggested such a link.

For the 14.5 survey, the effective depth (the maximum redshift at which an L^* galaxy is included in the survey) is ~ 5400 km s^{-1}; for the 15.5 survey, the effective depth is ~ 8500 km s^{-1}. Figure 9 shows the distribution of groups in the two surveys as a function of the mean velocity of the system. In the 14.5 survey, the median redshift of groups is 40% of the effective depth; in the 15.5 survey, the median redshift is 85% of the effective depth. As a consequence, most (58%) of the groups in the 15.5 survey contain three galaxies brighter than L^*. However, only 23% of the groups in the 14.5 survey have three members brighter than L^*. The systems in the two catalogs have significantly different intrinsic luminosities; for the luminosity function parameters of equation (12), 25% of the luminosity of a group is in galaxies brighter than L^*.

The difference in the median velocity dispersions for the two catalogs reflects the lack of a fair sample. The observed bubble- or spongelike structures in the 14.5 survey tend to be thinner (compare the nearby structures in Fig. 1 with the more distant ones) than the structures in the 15.5 survey. The thicker structures are undersampled or absent from the 14.5 survey. The 14.5 survey, although it covers about the same volume in redshift space as the 15.5 survey, is not sensitive to the largest structures present in the 15.5 survey. The effective depth of the 14.5 sample is just about equal to the diameter of the largest void in the 15.5 sample. The large angular scale coverage of the 14.5 survey does not compensate for the greater depth of the

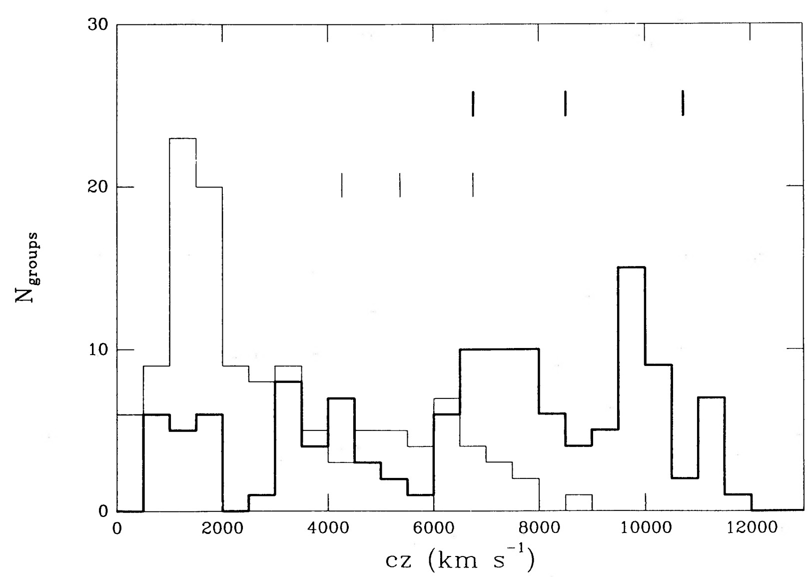

FIG. 9.—Number of groups as a function of redshift for the 14.5 sample (*light line*) and for the 15.5 sample (*heavy line*). The vertical lines mark the depths at which the apparent magnitude limits of the two surveys correspond to the absolute magnitudes $M^*_{B(0)} - 1$, $M^*_{B(0)}$ and $M^*_{B(0)} + 1$, respectively.

15.5 survey. Much of the information about large-scale structure in the 14.5 survey is redundant (see de Lapparent, Geller, and Huchra 1988).

VII. CONCLUSIONS

We apply an objective group identification algorithm (Huchra and Geller 1982) to the Center for Astrophysics redshift survey complete to $m_{B(0)} = 15.5$ over the right ascension range $8^h \leq \alpha \leq 17^h$ and declination range $26°.5 \leq \delta < 38°.5$. We extract a catalog of 128 groups with three or more members; 92 of these groups constitute our "statistical sample."

We use simulations of the geometry of large-scale structure to choose the selection for the identification algorithm. We identify a range where the survey contains more rich ($N_{\rm mem} \geq 5$) groups than the simulation and where the groups in the survey are stable to variation in the selection parameters. The groups have $\delta\rho/\rho = 80$ and $V_0 = 350$ km s^{-1}. For this group catalog, comparison with the simulations indicates that $\gtrsim 30\%$ of the groups with three or four members are probably accidental superpositions. These groups are a consequence of the geometry of large-scale structure; they are not necessarily the expected "fingers" in redshift space associated with physical systems of galaxies. Of course, it is not possible to distinguish the real groups from the accidental superpositions on the basis of these data.

One interesting issue beyond the scope of this paper is the behavior of the correlation function for individual galaxies which are not identified as group members. In other words, does the removal of "fingers" in velocity space remove the distortion observed in the correlation function, $\xi(R_p, \pi)$, of projected separation r_p and relative pairwise line-of-sight velocity π? For both the 14.5 and 15.5 samples the median velocity dispersion of groups is smaller than the expected $\sim 70\%$ of the rms pairwise peculiar velocity (de Lapparent, Geller, and Huchra 1988; Davis and Peebles 1983). The discrepancy may be merely a result of the different weighting of large systems with large velocity dispersions in the calculations of rms pairwise peculiar velocity relative to median group velocity dispersion.

The median velocity dispersion for the 36 groups in the "statistical sample" with five more members is $\sigma_v = 228$ km s^{-1}, and the median $M/L_{B(0)} = 178h\ M_\odot/L_\odot$. The median parameters for the 92 group sample are similar for the sample with $N_{\rm mem} \geq 5$. For this sample the critical mass-to-light ratio is $M/L_{\rm crit} = 1360h\ M_\odot/L_\odot$. If the mass-to-light ratios of groups are characteristic of the universe as a whole, the cosmological mean mass density Ω is equal to $0.13e^{\pm 0.9}$. The "error" in Ω comes from the quartile ranges in Table 6 and reflects the large spread in group mass-to-light ratios.

The 128 group sample contains seven Abell clusters; the physical properties of these clusters overlap substantially with those of groups. In fact, the distinction between groups and clusters is not generally apparent on the basis of selection of systems in redshift space. The similarity of group and cluster properties raises fundamental questions about the reliability of cluster catalogs as guides to systems with similar physical properties.

Comparison of the distribution of group centers with the distribution of all of the galaxies in the survey shows qualitatively that groups trace the large-scale structure in the region. We plan to examine this issue quantitatively by calculating the correlation function for the group centers. Perhaps comparison of the correlation functions for individual galaxies, groups, and clusters will lead to a resolution of the problems posed by the high amplitude of the cluster correlation function (see Bahcall and Soneira 1983; Geller 1987).

The physical properties of groups may be related to the details of the large-scale structure in the region. Groups extracted from the earlier CfA survey complete to $m_{B(0)} = 14.5$ have a significantly lower median velocity dispersion $\sigma_v = 131$ km s^{-1} in agreement with the previous results of NW. About 58% of the groups in the 15.5 survey contain three or more galaxies brighter than L^*; only 23% of the groups in the 14.5 survey have three or more bright members. The difference in the group catalogs is probably largely a result of the location of large-scale structures relative to the survey limits. The inhomogeneity of group properties probably reflects the large-scale inhomogeneity of the galaxy distribution.

We thank Valérie de Lapparent for providing the geometric models. We thank Ed Turner for entertaining discussions. This research was supported in part by NASA grant NAGW-201, by grants from the Smithsonian Institution, and by funds from the Italian Ministry of Education.

REFERENCES

Bahcall, N. A., and Soneira, R. M. 1983, *Ap. J.*, **270**, 20.
Davis, M., and Peebles, P. J. E. 1983, *Ap. J.*, **267**, 465.
de Lapparent, V. 1986, Ph.D thesis, University of Paris.
de Lapparent, V., Geller, M. J., and Huchra, J. P. 1988, *Ap. J.*, **332**, 44.
———. 1989, *Ap. J.*, **343**, 1.
de Vaucouleurs, G. 1975, in *Stars and Stellar Systems*, Vol. **9**, *Galaxies and the Universe*, ed. A. Sandage, M. Sandage, and J. Kristian (Chicago: University of Chicago Press), p. 557.
Faber, S. M., and Gallagher, J. S. 1979, *Ann. Rev. Astr. Ap.*, **17**, 135.
Geller, M. J. 1987, in *Large-Scale Structures in the Universe*, ed. L. Martinet and M. Mayor (Sauverny: Geneva Observatory), p. 71.
Geller, M. J., and Huchra, J. P. 1983, *Ap. J. Suppl.*, **52**, 61 (GH83).
Heisler, J., Tremaine, S., and Bahcall, J. N. 1985, *Ap. J.*, **298**, 8.
Holmberg, E. 1969, *Ark. Astr.*, **5**, 305.
Huchra, J. P., Davis, M., Latham, D., and Tonry, J. 1983, *Ap. J. Suppl.*, **52**, 39.
Huchra, J. P., and Geller, M. J. 1982, *Ap. J.*, **257**, 423 (HG82).
Huchra, J. P., Geller, M. J., de Lapparent, V., and Corwin, H. 1989, *Ap. J. Suppl.*, submitted.
Materne, J. 1978, *Astr. Ap.*, **63**, 401.
———. 1979, *Astr. Ap.*, **74**, 235.
Nolthenius, R., and White, S. D. M. 1987, *M.N.R.A.S.*, **225**, 505 (NW).
Press, W. H., and Davis, M. 1982, *Ap. J.*, **259**, 449.
Ramella, M., Geller, M. J., and Huchra, J. P. 1989, in preparation.
Rood, H. J., and Dickel, J. R. 1978, *Ap. J.*, **224**, 724.
Rood, H. J., Rothman, V. C. A., and Turnrose, B. E. 1970, *Ap. J.*, **162**, 411.
Schechter, P. 1976, *Ap. J.*, **203**, 297.
Tully, B. 1980, *Ap. J.*, **237**, 390.
———. 1987, *Ap. J.*, **321**, 280.
Turner, E. L., and Gott, J. R. 1976, *Ap. J. Suppl.*, **32**, 409.
Vennik, J. 1984, *Tartu Astr. Obs. Teated*, No. 73, p. 3.
Zabludoff, A., Huchra, J. P., and Geller, M. J. 1989, in preparation.
Zwicky, F. 1933, *Helv. Phys. Acta*, **6**, 10.

MARGARET J. GELLER and JOHN P. HUCHRA: Center for Astrophysics, 60 Garden Street, Cambridge, MA 02138

MASSIMO RAMELLA: Osservatorio Astronomico di Trieste, via G.B. Tiepolo, 11, I-34131 Trieste, Italy